metals

MDPI

Article

The Influence of Ultrasonic Vibration Frequency on the Properties of TiN Coated Biomedical Ti–13Zr–13Nb

A. Shah [1,*], S. Izman [2], Siti Nurul Fasehah Ismail [3], H. Mas Ayu [4], Che Ghani Che Kob [1], R. Daud [4] and Mohammed Rafiq Abdul Kadir [3]

1 Faculty of Technical and Vocational, Universiti Pendidikan Sultan Idris, 35900 Tanjong Malim, Perak, Malaysia; cheghani@ftv.upsi.edu.my
2 Faculty of Mechanical Engineering, Universiti Teknologi Malaysia, 81310 UTM Skudai, Johor, Malaysia; izman@utm.my
3 Faculty of Bioscience and Medical Engineering, Universiti Teknologi Malaysia, 81310 UTM Skudai, Johor, Malaysia; ezasesey_max@yahoo.com (S.N.F.I.); rafiq@biomedical.utm.my (M.R.A.K.)
4 Faculty of Mechanical Engineering, Universiti Malaysia Pahang, 26600 Pekan, Pahang, Malaysia; masszee@ump.edu.my (H.M.A.); rosdidaud@ump.edu.my (R.D.)
* Correspondence: armanshah@ftv.upsi.edu.my; Tel.: +605-450-5404

Received: 17 April 2018; Accepted: 2 May 2018; Published: 4 May 2018

Abstract: Bare biomedical grade titanium alloys are prone to degradation when in a body fluid environment. Surface coatings such as Physical Vapor Deposition (PVD) can serve as one of the options to minimize this issue. Past reports showed that the PVD coated layer consists of pores, pinholes, and columnar growths which act as channels through which the aggressive medium attacks the substrate. Duplex and multilayer coatings seem able to address this issue to varying extents but at the expense of manufacturing time and cost. In this paper, the effect of an ultrasonic vibration frequency on PVD TiN coated Ti–13Zr–13Nb biomedical alloy was studied. Disk type samples were prepared and coated with TiN at fixed conditions: bias voltage (−125 V), substrate temperature (300 °C), and nitrogen gas flow rate (300 standard cubic centimeters per minute (SCCM)). An ultrasonic vibration was then subsequently applied to the TiN coated samples at frequencies of 8 kHz and 16 kHz for 5 min. All TiN coated samples treated with ultrasonic vibrations exhibited a higher corrosion resistance than the untreated ones. Microstructure analysis under Field Emission Scanning Electron Microscopy (FESEM) confirmed that the coated sample at frequencies of 16 kHz produced the most compact coating. It is believed that the hammering effect of the ultrasonic vibration reduced the micro channels' size in the coating and thus decelerated the corrosion's attack.

Keywords: biomaterials; Ti–13Zr–13Nb; ultrasonic vibration; corrosion resistance; TiN; titanium alloy

1. Introduction

Titanium and its alloys are commonly used in biomedical applications as an implant for hip, knee, and shoulder replacements [1,2]. The selection of this material is due to its favorable characteristics such as biocompatibility, a low corrosion rate, low modulus, and a high strength to weight ratio as compared to other biomedical alloys (AISI 316L stainless steel, cobalt, and chromium alloys) [3–7]. Despite these advantages, titanium alloy has a major drawback: its high corrosion rate especially when in contact with body fluid [8]. It is well understood that the body environment is very aggressive owing to the presence of chloride ions and proteins. The corrosion of the implant releases toxic ions into the host body and causes inflammation which in some cases requires revision surgery [9]. This issue can be addressed to a large extent by applying a suitable surface coating or surface modification techniques.

Common surface modification techniques include Chemical Vapor Deposition (CVD) [10], Physical Vapor Deposition (PVD) [11–14], Ion Implantation [15], Plasma Spray coating [16], Sol Gel [17,18], Nitriding [19], and Thermal Oxidation [20,21]. Among these, the PVD technique shows promising results by offering a low processing temperature (<500 °C) over a wide range of coating thicknesses as compared to other methods. The processing temperature of other techniques is relatively high which restricts the type of potential substrates, as well as causing unexpected phase transitions and excessive residual stresses. Past reports showed that the PVD coated layer consists of pores, pinholes, and columnar growths which act as channels through which the aggressive medium attacks the substrate [22–27]. Duplex and multilayer coatings seem able to address this issue to varying extents but at the expense of manufacturing time and cost. Most of the researchers applied the chemical treatment to pinholes or columnar growths but very rarely used a mechanical treatment to solve this problem. The mechanical method is expected to improve the quality of the coated sample. Rodríguez-Barrero et al. reported that grinding was used to eliminate drag grinding. It found that grinding was a suitable final process for hard coatings in order to eliminate droplets, thereby achieving smooth, cutting edge surfaces [28]. Celaya et al. found that ultrasonic vibrations improved the surface quality of coated samples [29]. Therefore, a systematic method is needed to prevent the body fluids penetrating and reacting with the bare substrate. One of the possible surface modifications tried on PVD is an ultrasonic treatment with the presence of ball steel to make the coating more compact. In this work, the corrosion resistance of TiN after being subjected to the ultrasonic treatment at various ultrasonic vibration frequencies is evaluated in the presence of simulated body fluids.

2. Materials and Methods

The material used in this study was biomedical grade Ti–13Zr–13Nb with a chemical composition in wt % of: Nb: 14; Zr: 13.5; Fe: 0.05; C: 0.04; N: 0.02; H: 0.002; O: 0.10 and Ti: Balance. The material, received in rods, was cut into disks with a diameter of 10 mm and thickness of 2 mm using a precision cutter. Prior to the TiN coating, the substrates were cleaned ultrasonically in acetone for 30 min, then steam cleaned, finally being dried using a stream of compressed air. All substrates were mirror polished with SiC paper. The TiN was coated using a Cathodic Arc Physical Vapor Deposition (CAPVD) method. Titanium of 99.99% purity was used as the target in these experiments. Prior to the deposition, the substrates were subjected to metal ion etching for 5 min at −1000 V bias voltage. It was followed by the deposition process which was carried out under the following fixed parameters: the cathodic current was set at 100 A, the nitrogen gas flow rate at 300 standard cubic centimeters per minute (SCCM), the substrate temperatures at 300 °C, the substrate bias at −125 V, and the deposited time for 1 h. Field Emission Scanning Electron Microscopy (FESEM, Supra 35 VP, Carl Zeiss, Germany) was used for characterizing surface morphology. Electrochemical tests were carried out in Kokubo solution at 37 ± 0.1 °C using a conventional three-electrode cell governed by a potentiostat/galvanostat (Princeton Applied Research Model VersaSTAT 3 - 300). Saturated calomel (SCE) and graphite electrodes were used as a counter and reference electrode respectively. The samples were scanned at 0.6667 mV/s. Electrochemical impedance spectroscopy (EIS) was conducted to evaluate the corrosion mechanism between the substrate and coatings. Three conventional electrodes were also used in this study, which is similar to the Tafel plot. All procedure electrochemical tests were conducted at 37 °C in a Kokubo solution (pH 7.4). Impedance measurements were analyzed using a Frequency Response Analyzer (FRA). The spectrum was recorded using a frequency range between 10 kHz and 1 Hz. The applied alternating potential had a root mean square amplitude of 10 mV on the open circuit potential (OCP). In this study, the ultrasonic milling machine was used at 8 kHz and 16 kHz at holding of 5 min. Before the ultrasonic treatment was performed, the samples were mounted in the fixture, then the ball steel poured into to the fixture. The size of ball steel was about 200 µm. The fixture was located on a magnetic table and aligned straight to the ultrasonic tool (electrode). The z axis was fixed in order to prevent the excessive load and vibration causing damage to the sample.

3. Results and Discussion

Figure 1a–c show the SEM micrographs for ultrasonic treatments at 8 kHz and 16 kHz for 5 min exposure times when applied to TiN coated samples. This figure illustrates the different surface morphologies that occur when ultrasonic vibrations were applied for different ultrasonic vibration frequency. Regardless of ultrasonic vibration frequency, pinholes were observed on the substrate surface when ultrasonic treatments for 5 min were applied. In addition, more intense micro-droplet deformations were observed when the samples were subjected to ultrasonic treatments at 16 kHz. The number of pinholes decreased after 16 kHz compared to 8 kHz. It can be noted that as the ultrasonic vibration frequency increased from 8 kHz to 16 kHz, the coated sample became more deformed and had fewer pinholes. It is believed that penetration of ball steel into TiN coatings takes place at a higher ultrasonic frequency and thus the coating deform more locally. The deformation properties of the microdroplets fill up the pinholes and makes the surface smoother. It is also believed that loose microdroplets may be removed from the coating's surface while sticky microdroplets may be squeezed and deformed further into microchannels and pinholes.

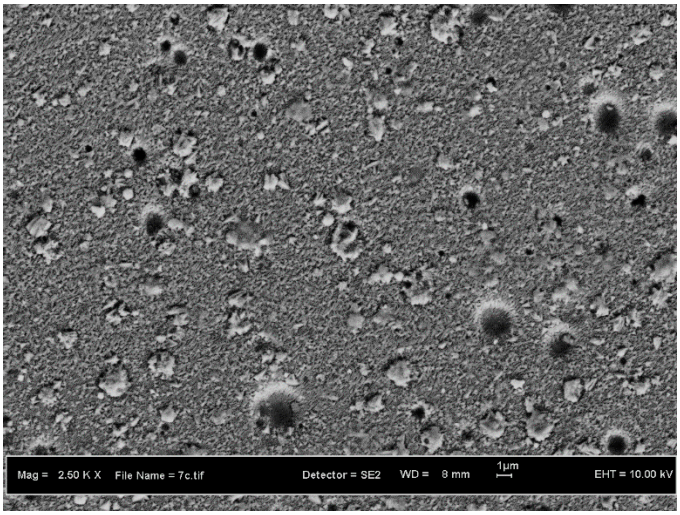

(**a**)

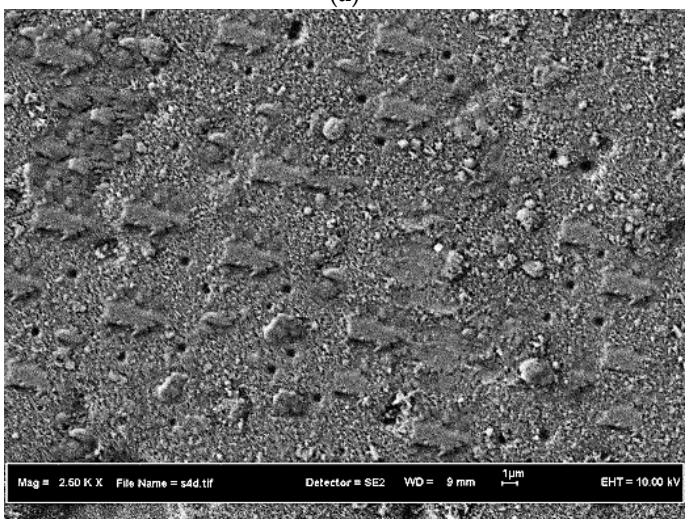

(**b**)

Figure 1. *Cont.*

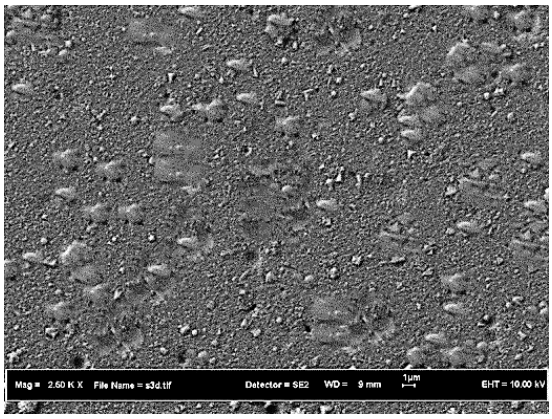

(**c**)

Figure 1. Surface morphology of TiN: (**a**) before ultrasonic treatment; (**b**) at 8 kHz; (**c**) at 16 kHz (ultrasonic treated for 5 min).

Figure 2a–c show cross sections of TiN coated samples after ultrasonic vibration at 8 kHz and 16 kHz after 5 min of exposure. No voids were observed and a uniform coating was apparent for all coated samples regardless of the ultrasonic vibration frequency. Figure 2 depicts the effect of ultrasonic treatment on the TiN coating thickness. As the ultrasonic vibration frequency increased to 16 kHz, the coating thickness decreased from 1.58 to 1.72 µm. Ultrasonic vibrations deformed the TiN coatings and reduced the coating thickness.

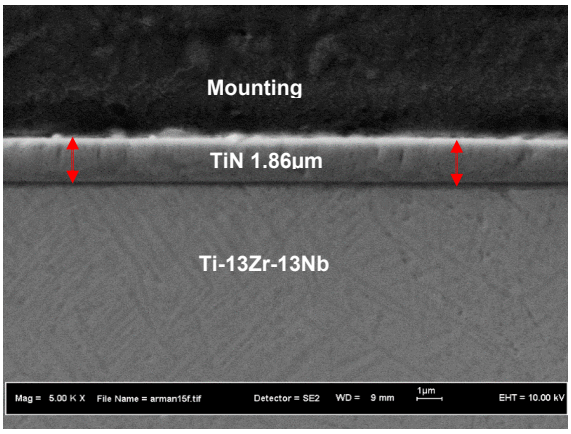

(**a**)

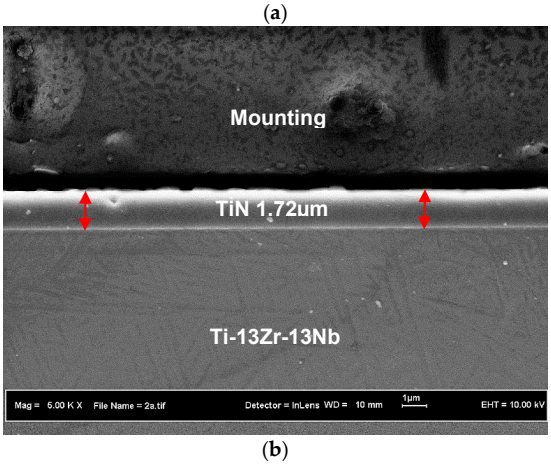

(**b**)

Figure 2. *Cont.*

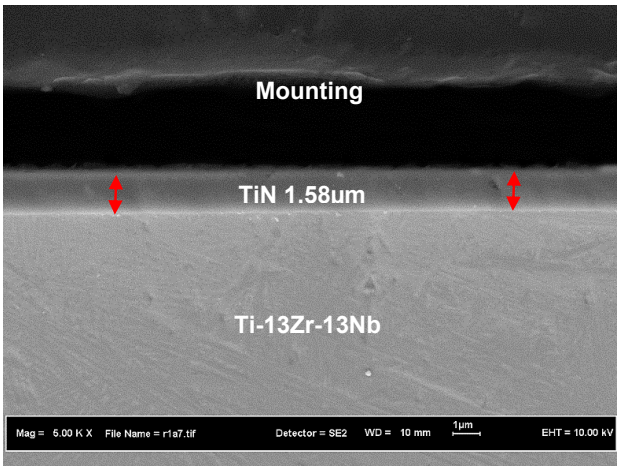

(**c**)

Figure 2. Cross-sectional view of TiN (**a**) before ultrasonic treatment, untrasonic treatment at (**b**) 8 kHz and (**c**) 16kHz.

The load vs. displacement plots showing the effect of ultrasonic treatments at 8 kHz and 16 kHz for 5 min on TiN coatings are illustrated in Figure 3. The plots for the samples that were not subjected to ultrasonic vibrations had higher indentation depths indicating they were softer than the coated samples treated with ultrasonic vibrations. The summary of the output data from nanoindentation tests is presented in Table 1. These results further confirm the findings provided by Figure 3. The hardness increased almost 1.5 times when an ultrasonic vibration frequency was applied to the sample at 8 kHz. The hardness increased by approximately 1.3 times when the ultrasonic vibration was increased from 8 kHz to 16 kHz. These results indicate that the increase in hardness when the ultrasonic frequency rose from 0 kHz to 8 kHz was more significant than the increase seen when the ultrasonic frequency increased from 8 kHz to 16 kHz. Table 1 also summarizes the resistance of the coated samples to plastic deformation as indicated by H^3/E^2. A better resistance to plastic deformation was noticed on the samples subjected to ultrasonic treatments. Additionally, resistance to plastic deformation increased as the ultrasonic frequency increased. The increase in H^3/E^2 when the ultrasonic treatment increased from 0 kHz to 8 kHz was more significant than the increase when the ultrasonic treatment rose from 8 kHz to 16 kHz. It is believed that increasing the hardness and elastic modulus of the samples increased the resistance of coated samples treated with ultrasonic vibrations to plastic deformation.

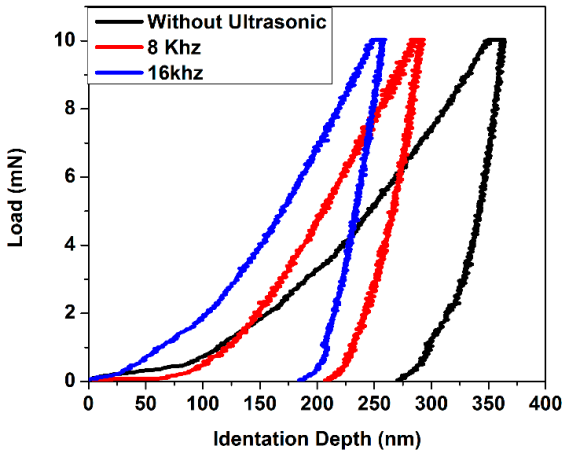

Figure 3. Load vs. displacement curve of TiN coated samples after ultrasonic treatment at 8kHz and 16 kHz.

Table 1. Summary of output data from the nanoindentation test for ultrasonic treatment at 16 kHz for different holding times.

Samples	Maximum Depth (nm)	Hardness (GPa)	Elastic Modulus, E (GPa)	H^3/E^2 Ratio
Without Ultrasonic	364.580	2.765	138.25	0.0011
8 kHz	286.876	4.210	165.78	0.0027
16 kHz	259.524	5.511	185.21	0.0049

Figure 4 uses a semi-logarithmic scale to depict the corrosion performance of ultrasonic treatments at 5 min exposure times for different ultrasonic vibration frequencies. The results indicated that an active passive transition was not apparent, suggesting the spontaneous formation of a passive film when the substrate was submerged in a Kokubo solution [30]. The corrosion current density of the coated samples subjected to ultrasonic vibrations shifted in a negative direction and displayed a leftward displacement in the anodic and cathodic branch of the curves (i.e., to lower current densities) compared to coated samples that were not subjected to ultrasonic vibrations. A similar phenomenon can be seen when the ultrasonic treatment increased from 8 kHz to 16 kHz. Coated samples with a higher ultrasonic frequency had greater corrosion resistance as compared to coated samples with a lower frequency. This result also indicates that ultrasonic vibrations had a significant effect on retarding the anodic dissolution of titanium alloy and inhibiting the cathodic hydrogen evolution reaction.

Table 2 summarizes the output data from Tafel plots. The ultrasonic frequency of 16 kHz has a lower corrosion current density and the corrosion rate was approximately 1.5 higher than it was for samples exposed to ultrasonic vibrations at only 8 kHz. Lower corrosion rates were attributed to the deformation of microdroplets and the reduction in the number of pinholes after longer exposure times. The SEM micrograph confirms this reduction in pinholes and micro-droplet deformation observed after longer exposure times.

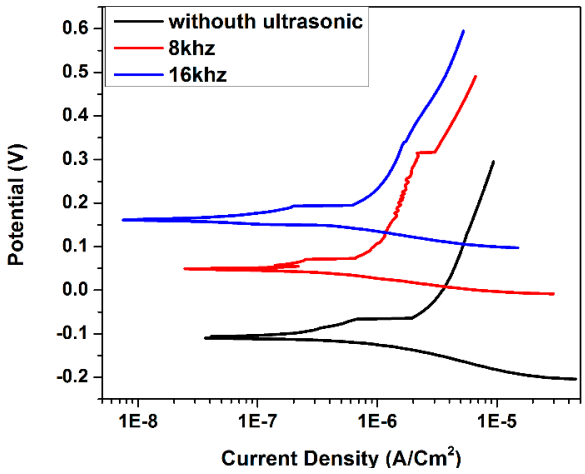

Figure 4. Tafel plots of TiN coated samples after ultrasonic treated at 8 kHz and 16 kHz.

Figure 5 shows the Nyquist plot for ultrasonic vibration parameters on the TiN coating. It is revealed that the ultrasonic vibration at various ultrasonic frequencies significantly improves corrosion resistance as compared to samples without ultrasonic treatment. In addition, it is also observed that the impedance of the samples treated with ultrasonic vibrations increased from 2816 to 3766 Charge of Transfer Resistance (Rct) as the ultrasonic frequency increased. It can be said that the higher ultrasonic frequency the higher the corrosion resistance as compared to those at lower ultrasonic frequencies.

Bode Plots (log |z| Vs log f and Phase angle Vs log f) for the ultrasonic treatment with different ultrasonic frequencies are shown in Figure 6a,b, respectively. It can be seen in Figure 6a that the total impedance as indicated by |z| is higher at ultrasonic frequency 16 kHz as compared to those

samples which underwent ultrasonic treatment at 8 kHz. It is clearly seen in Figure 6b that the two times constant appears which is indicating the interface between the solution/TiN and TiN/substrate. The equivalent circuit is proposed based on data plotted on Nyquist and both bode plots which are presented in Figure 7. The output data from EIS are given in Table 2. It was found that the R_{ct} for the ultrasonic frequency of 16 kHz was 1.5 times higher than the sample treated at 8 kHz. It also can be noticed that while the R_{ct} values increase with the exposure time, the C_{dl} values decrease, indicating the formation of a surface film. This result is quite commonly found by EIS and the explanation for this phenomenon has been discussed previously.

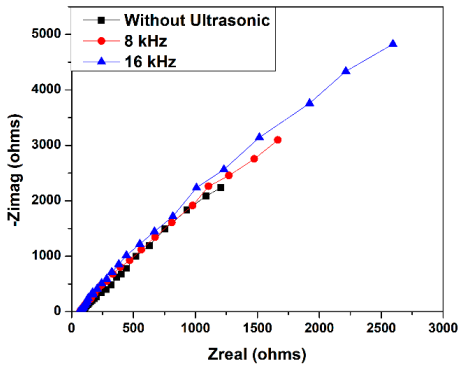

Figure 5. Nyquist plots for TiN coated samples after ultrasonic treated at 8 kHz and 16 kHz.

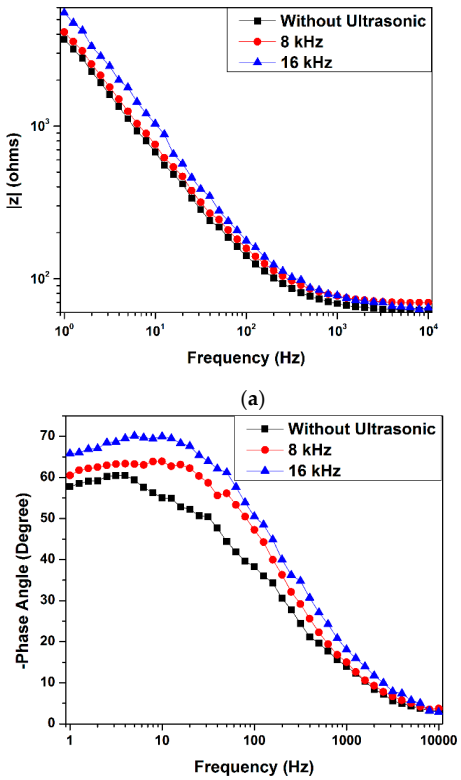

Figure 6. Bode Plots: (**a**) log |z| Vs log f and; (**b**) phase angle Vs log f for ultrasonic treated on TiN coatings at 8 kHz and 16 kHz for various holding times.

Table 2. Corrosion parameters calculated from Tafel and electrochemical impedance spectroscopy (EIS) for ultrasonic treatment on TiN coating at 8kHz and 16 kHz for different holding times.

Samples	Ecorr (mv)	Icorr ($\mu A/cm^2$)	Corrosion Rate (mm/Year)	R_{ct}	C_{dl}
Without Ultrasonic	−110.11	0.971	18.6323×10^{-3}	1883	2.7×10^{-5}
8 kHz	49.07	0.261	4.9241×10^{-3}	2816	1.73×10^{-5}
16 kHz	−122.07	0.185	3.7843×10^{-3}	3766	8.8×10^{-6}

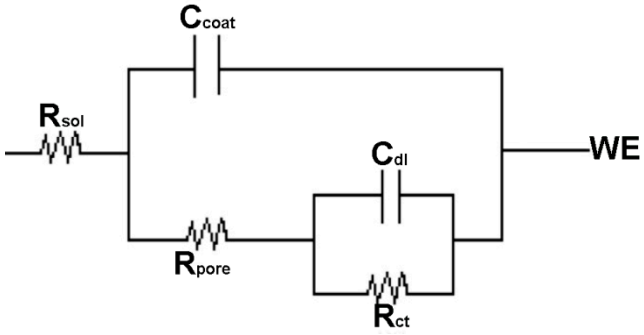

Figure 7. Equivalent circuit to fit electrochemical impedance data.

4. Conclusions

The following conclusions can be drawn from this experimental study:

I. Ultrasonic frequency effects on TiN coating properties after subjected with ultrasonic treatment were noted: as the ultrasonic frequency increased, the more intense the coating deformation, the less the number of microdroplets, the less the coating thickness, and the higher the coating's hardness.

II. It was found that the corrosion properties of the TiN coating significantly improved after treated with ultrasonic vibrations. It seems that the ultrasonic vibration was able to deform the coating and fill up the pinholes thus improving the corrosion resistance of the coated sample. Charge transfer resistance and current density increased from 2816 to 3766 and 0.261 to 0.185, respectively, when the ultrasonic frequency increased. This indicates that there was less penetration from the simulated body fluids into the coating due to the compactness of the coating properties created at extreme conditions using the ultrasonic treatment.

Author Contributions: For A.S., M.R.A.K. and S.I. designed most experiments, analyzed the results and wrote this manuscript. M.A. and R.D. performed most experiments. C.G. and C.K. and S.N.F.I. helped analyze the experimental data and gave some constructive suggestions about how to write this manuscript.

Acknowledgments: The authors would like to express their highest gratitude to the Ministry of Higher Education and Universiti Pendidikan Sultan Idris (UPSI) for the funding of this research project (Fundamental Research Grant Schem FRGS) via code number 2016-0067-104-02. Thanks also to Universiti Kebangsaan Malaysia (UKM) for funding the Regional Cluster Research Publication (RCRP code -2017-0043-104-61).

Conflicts of Interest: The authors declare no conflict of interest.

References

1. Gonzalez, E.D.; Afonso, C.R.M.; Nascente, P.A.P. Influence of Nb content on the structure, morphology, nanostructure, and properties of titanium-niobium magnetron sputter deposited coatings for biomedical applications. *Surf. Coat. Technol.* **2017**, *326*, 424–428. [CrossRef]
2. Wang, P.; Wu, L.; Feng, Y.; Bai, J.; Zhang, B.; Song, J.; Guan, S. Microstructure and mechanical properties of a newly developed low young's modulus Ti–15Zr–5Cr–2Al biomedical alloy. *Mater. Sci. Eng. C* **2017**, *72*, 536–542. [CrossRef] [PubMed]

3. Abboud, J.H. Effect of processing parameters on titanium nitrided surface layers produced by laser gas nitriding. *Surf. Coat. Technol.* **2013**, *214*, 19–29. [CrossRef]
4. Ohtsu, N.; Nakamura, Y.; Semboshi, S. Thin hydroxyapatite coating on titanium fabricated by chemical coating process using calcium phosphate slurry. *Surf. Coat. Technol.* **2012**, *206*, 2616–2621. [CrossRef]
5. Zhao, B.H.; Zhang, W.; Wang, D.N.; Feng, W.; Liu, Y.; Lin, Z.; Du, K.Q.; Deng, C.F. Effect of Zn content on cytoactivity and bacteriostasis of micro-arc oxidation coatings on pure titanium. *Surf. Coat. Technol.* **2012**, *228*, S428–S432. [CrossRef]
6. Wu, J.; Li, H.; Yuan, B.; Gao, Y. High recoverable strain tailoring by Zr adjustment of sintered Ti–13Nb–(0–6)Zr biomedical alloys. *J. Mech. Behav. Biomed.* **2017**, *75*, 574–580. [CrossRef] [PubMed]
7. Xiao, M.; Chen, Y.M.; Biao, M.N.; Zhang, X.D.; Yang, B.C. Bio-functionalization of biomedical metals. *Mater. Sci. Eng. C* **2017**, *70*, 1057–1070. [CrossRef] [PubMed]
8. Shah, A.; Izman, S.; Abdul-Kadir, M.R.; Ayu, H.M.; Anwar, M.; Ma'aram, A. Influence of bias voltage on corrosion resistance of TiN coated on biomedical TiZrNb alloy. *Adv. Mater. Res.* **2014**, *845*, 436–440. [CrossRef]
9. Geetha, M.; Singh, A.K.; Asokamani, R.; Gogia, A.K. Ti based biomaterials, the ultimate choice for orthopaedic implants—A review. *Prog. Mater. Sci.* **2009**, *54*, 397–425. [CrossRef]
10. Mohan, L.; Anandan, C.; Grips, V.K.W. Corrosion behavior of titanium alloy Beta-21s coated with diamond like carbon in Hank's solution. *Appl. Surf. Sci.* **2012**, *258*, 6331–6340. [CrossRef]
11. Shah, A.; Izman, S.; Fasehah, S.N. Study on micro droplet reduction on TiN coated biomedical Ti–13Zr–13Nb alloy. *J. Teknol.* **2016**, *78*, 1–5. [CrossRef]
12. Shah, A.; Izman, S.; Hassan, M.A. Influence of nitrogen flow rate in reducing TiN microdroplets on biomedical Ti–13Zr–13Nb alloy. *J. Teknol.* **2016**, *78*, 6–10. [CrossRef]
13. Shah, A.; Izman, S.; Abdul-Kadir, M.R.; Mas-Ayu, H. Influence of substrate temperature on adhesion strength of TiN coating of biomedical Ti–13Zr–13Nb alloy. *Arab. J. Sci. Eng.* **2017**, *42*, 4737–4742. [CrossRef]
14. Shah, A.; Izman, S.; Ismail, S.N.F.; Mas-Ayu, H.; Daud, R. Study on adhesion strength of TiN coated biomedical Ti–13Zr–13Nb alloy. *J. Teknol.* **2018**, *80*, 27–35. [CrossRef]
15. Hongxi, L.; Qian, X.; Xiaowei, Z.; Chuanqi, W.; Baoyin, T. Wear and corrosion behaviors of Ti6Al4V alloy biomedical materials by silver plasma immersion ion implantation process. *Thin Solid Films* **2012**, *521*, 89–93. [CrossRef]
16. Sathish, S.; Geetha, M.; Aruna, S.T.; Balaji, N.; Rajam, K.S.; Asokamani, R. Sliding wear behavior of plasma sprayed nanoceramic coatings for biomedical applications. *Wear* **2011**, *271*, 934–941. [CrossRef]
17. Ayu, H.M.; Izman, S.; Daud, R.; Krishnamurithy, G.; Shah, A.; Tomadi, S.H.; Salwani, M.S. Surface Modification on CoCrMo Alloy to Improve the Adhesion Strength of Hydroxyapatite Coating. *Procedia Eng.* **2017**, *184*, 399–408. [CrossRef]
18. Mas Ayu, H.; Izman, S.; Daud, R.; Shah, A.; Anwar, M.; Krishnamurithy, G.; Kamarul, T. In Vitro biocompatibility study of hydroxyapatite coated on Co-Cr-Mo with oxide interlayer. *J. Teknol.* **2018**, *80*, 35–42. [CrossRef]
19. Raoufi, M.; Mirdamadi, S.; Mahboubi, F.; Ahangarani, S.; Mahdipoor, M.S.; Elmkhah, H. Effect of active screen plasma nitriding pretreatment on wear behavior of TiN coating deposited by PACVD technique. *Appl. Surf. Sci.* **2012**, *258*, 7820–7825. [CrossRef]
20. Izman, S.; Shah, A.; Abdul-Kadir, M.R.; Nazim, E.M.; Anwar, M.; Hassan, M.A.; Safari, H. Effect of thermal oxidation temperature on rutile structure formation of biomedical TiZrNb alloy. *Adv. Mater. Res.* **2012**, *393*, 704–708. [CrossRef]
21. Mas-Ayu, H.; Izman, S.; Abdul-Kadir, M.R.; Daud, R.; Shah, A.; Yusoff, M.F.M.; Shamsiah, M.W.; Yong, T.M.; Kamarul, T. Influence of carbon concentrations in reducing Co and Cr ions release in cobalt based implant: A preliminary report. *Adv. Mater. Res.* **2014**, *845*, 462–466. [CrossRef]
22. Subramanian, B.; Jayachandran, M. Electrochemical corrosion behavior of magnetron sputtered TiN coated steel in simulated bodily fluid and its hemocompatibility. *Mater. Lett.* **2008**, *62*, 1727–1730. [CrossRef]
23. Ali, A.; Ahmad, A.; Deen, K.M. Multilayer ceramic coating for impeding corrosion of sintered NdFeB magnets. *J. Rare Earths* **2009**, *27*, 1003–1007. [CrossRef]
24. Tian, R. Chromium Nitride/Cr coated 316l stainless steel as bipolar plate for proton exchange membrane fuel cell. *J. Power Sources* **2011**, *196*, 1258–1263. [CrossRef]

25. Bobzin, K.; Bagcivan, N.; Theiß, S.; Weiß, R.; Depner, U.; Troßmann, T.; Ellermeier, J.; Oechsner, M. Behavior of DLC coated low-alloy steel under tribological and corrosive load: Effect of top layer and interlayer variation. *Surf. Coat. Technol.* **2013**, *215*, 110–118. [CrossRef]
26. Mutyala, K.C.; Ghanbari, E.; Doll, G.L. Effect of deposition method on tribological performance and corrosion resistance characteristics of CrXn coatings deposited by physical vapor deposition. *Thin Solid Films* **2017**, *636*, 232–239. [CrossRef]
27. Zhang, B.; Wei, L.; Gao, L.; Guo, H.; Xu, H. Microstructural characterization of PS-PVD ceramic thermal barrier coatings with quasi-columnar structures. *Surf. Coat. Technol.* **2017**, *311*, 199–205. [CrossRef]
28. Rodríguez-Barrero, S.; Fernández-Larrinoa, J.; Azkona, I.; López De Lacalle, L.N.; Polvorosa, R. Enhanced performance of nanostructured coatings for drilling by droplet elimination. *Mater. Manuf. Process.* **2016**, *31*, 593–602. [CrossRef]
29. Celaya, A.; De Lacalle, L.N.L.; Campa, F.J.; Lamikiz, A. Ultrasonic assisted turning of mild steels. *Int. J. Mater. Prod. Technol.* **2010**, *37*, 60–70. [CrossRef]
30. Suresh, K.S.; Geetha, M.; Richard, C.; Landoulsi, J.; Ramasawmy, H.; Suwas, S.; Asokamani, R. Effect of equal channel angular extrusion on wear and corrosion behavior of the orthopedic Ti–13Nb–13Zr alloy in simulated body fluid. *Mater. Sci. Eng. C* **2012**, *32*, 763–771. [CrossRef]